

Spin Dependence in the Excitation of the First 2^+ State of $^{54}\text{Fe}^\dagger$

J. R. Tesmer* and F. H. Schmidt

University of Washington, Seattle, Washington 98105

(Received 29 January 1971)

Proton- γ angular-correlation measurements at 19.6 MeV, together with asymmetry data for excitation of the first 2^+ state of ^{54}Fe , yield strong evidence for the full Thomas form of the spin-dependent collective-coupling potential. In addition, the agreement between these data and calculations is improved when the spin-dependent deformation $\beta_{s.o.}$ is twice β_2 , the deformation parameter for the central potential.

Inelastic scattering of 19.6-MeV protons from the first excited 2^+ state of ^{54}Fe has been studied extensively. Proton- γ angular-correlation measurements of both the in-plane¹ and the z -axis or spin-flip^{2,3} types have been reported. Inelastic asymmetry experiments were performed at Saclay.²

It has been observed that the asymmetry data for ^{54}Fe could not be matched by the collective model in the distorted-wave Born approximation (DWBA) with $\beta_{s.o.} = \beta_2$, whereas good agreement was found for both ^{56}Fe and ^{58}Ni .⁴ Sherif and Blair⁵ have proposed an increase in $\beta_{s.o.}$ to improve asymmetry predictions, and recently Raynal⁶ showed that with $\beta_{s.o.}$ equal to 2 or 3 times β_2 , the ^{54}Fe asymmetry at 18.6 MeV could be reasonably well matched. On the other hand, spin-flip data for ^{54}Fe and ^{56}Fe are very similar but cannot be predicted in detail.² These results seem contradictory since both asymmetry and spin flip depend upon the spin-dependent interactions.

In this Letter we point out that the in-plane correlation data, in conjunction with spin-flip measurements, provide a sensitive test of the form for the spin-dependent perturbation, or coupling, potential which causes the transition. These data also lend substantial support for setting $\beta_{s.o.} = 2\beta_2$ for this coupling potential in the case of ^{54}Fe at 19.6 MeV. We also discuss a physical interpretation of the scattering process in a manner which leads to greater insight. Finally, we mention further experimental studies which could help resolve unanswered questions.

The coincident quadrupole-radiation intensity in the plane of a proton reaction due to a $2^+ \rightarrow 0^+$ transition has a familiar five-parameter normalized form (see, e.g., Schmidt *et al.*⁷) which is independent of the reaction mechanism, viz.,

$$W(\varphi_\gamma, \varphi_p) = (5/16\pi)[A + B \sin^2(\varphi_\gamma - \epsilon_1) + C \sin^2 2(\varphi_\gamma - \epsilon_2)],$$

where φ_γ and φ_p are the emission and scattering

angles for the γ ray and the proton, respectively. The five experimentally determinable parameters, A , B , C , ϵ_1 , and ϵ_2 , contain the magnitude of the amplitudes and their phases for excitation of the quantum substates which make up the 2^+ state. (Explicit formulas are given in Ref. 7.) For example, $a_m(\uparrow\uparrow) \exp[i\beta_m(\uparrow\uparrow)]$ is the amplitude for excitation of the m th substate by protons whose spin goes from "up" to "down." If we choose our quantization axis perpendicular to the reaction plane, then the Bohr theorem⁸ assures us that the pair of states $m = \pm 1$ interfere incoherently with the pair $m = \pm 2$, and that the $m = \pm 1$ states arise only through proton spin flip. Also, since we could in principle distinguish between ($\uparrow\uparrow$) and ($\uparrow\downarrow$) scattering experimentally, these processes interfere incoherently.

The origins of the parameters B , C , ϵ_1 , and ϵ_2 are as follows: B arises from spin flip; it can nevertheless be zero if (say) only the $m = \pm 1$ state is excited. ϵ_1 is related to the phase difference between $m = +1$ and -1 states. C and ϵ_2 are similar quantities for the $m = +2$ and -2 states. The $m = 0$ state does not contribute to the in-plane radiation. The significance of the parameter A will be discussed below.

We have found experimentally that A is nearly zero for scattering angles in $^{54}\text{Fe}(p, p'\gamma)$ in the forward direction and then exhibits a back-angle peak, as shown in Fig. 1(a). The spin-flip probability, S_1 , has a similar back-angle peak [Fig. 1(b)].

The parameter A contains all the amplitudes except those for the $m = 0$ state. We first examine the conditions under which it can be zero, as is approximately the case for forward scattering: (1) The equalities $a_{+2}(\uparrow\uparrow) = a_{-2}(\uparrow\uparrow)$, $a_{+2}(\uparrow\downarrow) = a_{-2}(\uparrow\downarrow)$, $a_{+1}(\uparrow\uparrow) = a_{-1}(\uparrow\uparrow)$, and $a_{+1}(\uparrow\downarrow) = a_{-1}(\uparrow\downarrow)$ must hold; (2) the difference in phase angles, $\beta_{+2}(\uparrow\uparrow) - \beta_{-2}(\uparrow\uparrow)$, must equal the difference $\beta_{+2}(\uparrow\downarrow) - \beta_{-2}(\uparrow\downarrow)$, and similarly for the ± 1 states. The first condition assures full coherent cancellation of the plus and minus substates along the radia-

tion symmetry axes, and the second provides symmetric incoherent overlap of these two patterns. Note, however, that $a_{\pm 2,0}(\uparrow\uparrow)$ may be different from $a_{\pm 2,0}(\uparrow\downarrow)$, etc. It is just these differences which will contribute to asymmetry in scattering with a polarized beam. Similar contributions can arise from $a_{\pm 1}(\uparrow\downarrow)$ and $a_{\pm 1}(\uparrow\uparrow)$.

From the experimental data shown in Figs. 1(a) and 1(b), we conclude that in the forward direction, where both A and S_1 are very small, the predominant scattering amplitudes are the a_0 's and the a_2 's. Thus both the equalities expressed by conditions (1) and (2) hold approximately. The equalities of condition (2) for the $m = +2$ and -2 states are further supported by the experimental behavior of ϵ_2 (not illustrated), which follows closely the adiabatic recoil axis. In the adiabatic approximation A is zero for α -particle scattering.⁹ Since $(\uparrow\uparrow)$ and $(\uparrow\downarrow)$ processes do not interfere coherently, we may think of each of these as α -particlelike scatterings. When condition (2) is met, these two radiation patterns coincide and make A zero. Hence, the fact that ϵ_2 exhibits adiabatic behavior supports equality of these phase-angle differences. The inelastic asymmetry in the forward direction, as shown in Fig. 1(c), arises primarily from a difference between $(\uparrow\uparrow)$ and $(\uparrow\downarrow)$ in the $m = \pm 2, 0$ substates.

In the backward direction both A and S_1 have a pronounced peak. It is therefore probable that the peak in A arises from the spin-flip amplitudes, so that either one or both of the equality conditions (1) and (2) for the $m = \pm 1$ states does not hold. Our data concerning the angle ϵ_1 are rather poor, and it is difficult to argue as we did above for ϵ_2 .

We next compare the experimental results for the asymmetry S_1 and A with collective-model DWBA calculations performed with the code developed by Sherif.¹⁰ The standard optical-model parameters of Becchetti and Greenlees were used.¹¹

The various predictions are shown on the figures. The curves are for different forms and strengths of the spin-dependent coupling potential $\Delta U_{s.o.}$. Two forms for this potential are employed: Those labeled OR use the unsymmetrized form of the potential suggested by the Oak Ridge group,¹² and the predictions labeled FT use the full Thomas form proposed by Sherif and Blair.⁵ These two forms are

$$\Delta U_{s.o.}(\text{OR}) = \left(\frac{\hbar}{m_\pi c}\right)^2 V_{s.o.} \alpha_{s.o.}(\hat{r}) \frac{1}{r} \frac{\partial}{\partial r} \frac{\partial f}{\partial R_{s.o.}} \vec{\sigma} \cdot \vec{L},$$

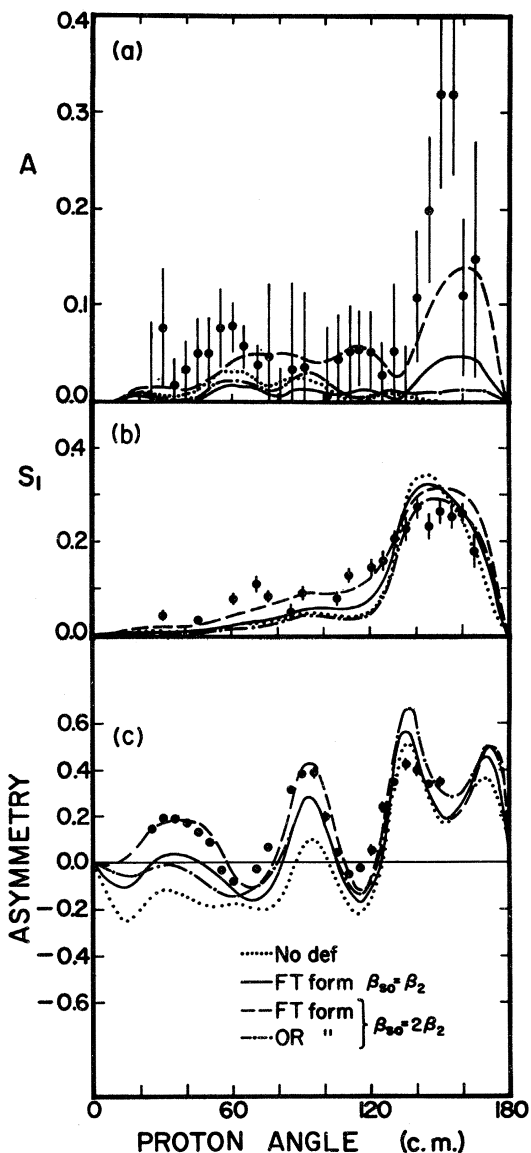


FIG. 1. (a) The parameter A for the in-plane correlation function; (b) the spin-flip probability S_1 as determined by z -axis correlation measurements; (c) the inelastic asymmetry. The curves are drawn for various DWBA calculations as described in the text.

and

$$\Delta U_{s.o.}(\text{FT}) = \Delta U_{s.o.}(\text{OR}) + \left(\frac{\hbar}{m_\pi c}\right)^2 V_{s.o.} \frac{\partial f}{\partial R_{s.o.}} \vec{\sigma} \cdot \nabla [\alpha_{s.o.}(\hat{r})] \times \frac{\nabla}{i}.$$

In these expressions, $f \equiv f(r, a_{s.o.}, R_{s.o.})$ is the Woods-Saxon form factor, where $a_{s.o.}$ and $R_{s.o.}$ are the diffuseness and radius parameters, respectively, of the spin-dependent term of the optical potential; and $\alpha_{s.o.}(\hat{r})$ is the spin-dependent

deformation and is defined by

$$\langle IM | \alpha_{s\Omega}(\hat{\varphi}) | 00 \rangle = \beta_{s\Omega} R_{s\Omega} Y_I^{M*}(\hat{\varphi}) [I+1]^{-1/2},$$

where $|IM\rangle$ and $|00\rangle$ are the initial and final nuclear states, respectively, and $\beta_{s\Omega}$ is the deformation parameter.

In addition to employing the two forms for $\Delta U_{s\Omega}$ we have varied its strength by assigning different values to $\beta_{s\Omega}$. It is customary to set $\beta_{s\Omega} = \beta_2$, the deformation parameter for the central potential. For the curves labeled "No def," $\beta_{s\Omega} = 0$; i.e., $\Delta U_{s\Omega} = 0$, so there is no spin-dependent coupling (but spin-dependent forces still act in the elastic channels). Calculations are also shown for $\beta_{s\Omega} = \beta_2$, and $\beta_{s\Omega} = 2\beta_2$. It is important to note that the latter does not necessarily imply a greater deformation of the spin-dependent potential; it is only a convenient means for increasing the strength of the spin-dependent force for exciting the state.

Three clear conclusions can be drawn from a comparison of the various predictions with the three sets of experimental data: (1) The full Thomas form is superior, especially with regard to the parameter A . (2) $\beta_{s\Omega} = 2\beta_2$ is also superior and improves the fit to A and to the asymmetry. (3) The fit to the spin flip is somewhat better with the FT form and with $\beta_{s\Omega} = 2\beta_2$, as is also the case for ^{58}Ni .¹³ Sherif and Blair⁵ proposed an increase in $\Delta U_{s\Omega}$ as a means of improving asymmetry predictions. As noted above, Raynal⁶ found this to be effective for ^{54}Fe at 18.6 MeV. He bases his argument upon a microscopic description in cases where there is an open proton shell and a closed neutron shell, which is the case for ^{54}Fe .

A comparison between the various calculations shows that S_1 is but little affected by $\beta_{s\Omega}$. The chief contributor to S_1 , which is the sum of spin-flip processes, thus lies in the distortion of the elastic waves generated by the central spin-dependent potential. This conclusion seems to hold for other targets as well. On the other hand, if the amplitudes for $(\uparrow\uparrow)$ were different from those for $(\uparrow\downarrow)$, we would expect to observe a spin-flip asymmetry in scattering performed with a polarized beam. In analogy with inelastic asymmetries, spin-flip asymmetry should be sensitive to $\beta_{s\Omega}$. Lowe¹⁴ has measured spin flip with a polarized beam for ^{12}C . Experimental difficulties preclude drawing clear conclusions, but there is some indication of an asymmetry. Measurements of the parameter A with a polarized beam, though more difficult, would contribute

further insight into the scattering process.

In our discussion of the back-angle peak in A , we suggested that the contributions to A are primarily due to differences between a_{+1} and a_{-1} , and/or to phase-angle differences. We have examined these amplitudes as predicted by the computer calculation, and find that these differences are primarily due to the $m = \pm 1$ phase differences, rather than to $a_{+1} \neq a_{-1}$.

The superiority of the full Thomas form of $\Delta U_{s\Omega}$ has been evident in the measurements of inelastic asymmetries for some time, but the improvement is most dramatic for bombarding energies higher than 20 MeV. The pronounced effect on the parameter A for the data at 19.6 MeV constitutes clear evidence of the superiority of the FT form for lower energies as well. Thus, the parameter A apparently pins down the form of $\Delta U_{s\Omega}$, while the asymmetry determines the magnitude of $\Delta U_{s\Omega}$. Since the asymmetries for ^{56}Fe and ^{58}Ni are adequately explained by $\beta_{s\Omega} = \beta_2$, it would appear that these 2^+ states do not require $\beta_{s\Omega} \neq \beta_2$.

We are deeply indebted to Donald M. Patterson, Jüri Eenmaa, Thomas K. Lewellen, Phyllis A. Russo, and members of the Laboratory staff for help with the data collection. We also wish to thank Professor John S. Blair and Professor Ernest M. Henley for many helpful comments.

†Research supported in part by the U. S. Atomic Energy Commission.

*Present address: Department of Physics, Purdue University, Lafayette, Ind. 47907.

¹J. R. Tesmer, J. Eenmaa, T. Lewellen, D. M. Patterson, P. A. Russo, and F. H. Schmidt, Bull. Amer. Phys. Soc. **15**, 1680 (1970).

²D. L. Hendrie, C. Glashauser, J. M. Moss, and J. Thirion, Phys. Rev. **186**, 1188 (1969). Asymmetry data given in this reference were provided by B. Mayer and J. Thirion (Saclay).

³J. R. Tesmer, thesis, University of Washington, 1971 (unpublished).

⁴C. Glashauser, R. de Swiniarski, and J. Thirion, Phys. Rev. **164**, 1437 (1967).

⁵H. Sherif and J. S. Blair, Phys. Lett. **26B**, 489 (1968).

⁶J. Raynal, in Proceedings of the Third International Symposium on Polarization Phenomena of Nucleons, Madison, Wis., 1970 (to be published).

⁷F. H. Schmidt, R. E. Brown, J. B. Gerhart, and W. A. Kolasinski, Nucl. Phys. **52**, 353 (1964).

⁸A. Bohr, Nucl. Phys. **10**, 486 (1959).

⁹J. S. Blair and L. Wilets, Phys. Rev. **121**, 1493 (1961).

¹⁰H. Sherif, thesis, University of Washington, 1968 (unpublished).

¹¹F. D. Becchetti, Jr., and G. W. Greenlees, Phys. Rev. **182**, 1190 (1969).

¹²M. P. Fricke, R. M. Drisko, R. H. Bassel, E. E. Gross, B. J. Morton, and A. Zucker, Phys. Rev. Lett. **16**, 746 (1966).

¹³J. Eenmaa, F. H. Schmidt, and J. R. Tesmer, Phys. Lett. **26B**, 321 (1968).

¹⁴J. Lowe, M. Ahmed, P. M. Rolph, and V. Hnizdo, Bull. Amer. Phys. Soc. **15**, 521 (1970), and private communication.

Total Cross Sections for $\pi^-p \rightarrow \Lambda K^0$ from Threshold to 1.13 GeV/c*

J. J. Jones,[†] T. Bowen, W. R. Dawes,[‡] D. A. DeLise,[§] E. W. Jenkins, R. M. Kalbach
E. I. Malamud,^{||} K. J. Nield, and D. V. Petersen

Department of Physics, University of Arizona, Tucson, Arizona 85721

(Received 24 November 1970)

Total cross sections for $\pi^-p \rightarrow \Lambda K^0$ have been measured using optical spark chambers from threshold to 1.13-GeV/c beam momentum in 19-MeV/c intervals, but with a 1-MeV/c resolution in the regions of the ΛK and ΣK thresholds. The behavior near ΛK threshold indicates a significant *s*-wave contribution, but this experiment is unable to resolve any cusplike behavior in the region of the ΣK thresholds. The cross section shows a broad peak in the vicinity of 1.05-GeV/c beam momentum.

A number of experimental studies have been made of the momentum dependence of the total cross section for the reaction $\pi^-p \rightarrow \Lambda K^0$ in the region of incident pion momentum extending from threshold up to and beyond that corresponding to the thresholds for $\Sigma^0 K^0$ and $\Sigma^- K^+$ production.¹⁻⁸ These studies have sought to clarify the mechanism for ΛK production near threshold, to search for new resonances, and to find evidence for the predicted cusplike behavior of the total cross section in the region of the ΣK thresholds. A limitation in previously published studies has been imposed by the uncertainty in the incident pion momentum, typically $\pm 2\%$, which places a lower limit on the characteristic width of detectable structure of ~ 20 MeV/c. In the present experiment, the width of detectable structure in the momentum dependence of the total cross section for ΛK production is reduced to ± 1 MeV/c by the use of a spark-chamber spectrometer in the incident pion beam. This apparatus, described elsewhere,⁹ permits determination of the momentum of individual incident pions with a relative precision better than $\pm 0.1\%$, and with an absolute calibration obtained from kinematic event fitting near the $\Lambda^0 K^0$ and $\Sigma^0 K^0$ thresholds.

The present experiment employed a secondary pion beam of the Lawrence Radiation Laboratory Bevatron whose central momentum was adjusted from 0.910 to 1.135 GeV/c with a momentum spread at any setting of approximately 2%. After passing through the spectrometer, this beam was focused on a 1-in.-thick liquid-hydrogen target. An array of spark chambers located upstream

and downstream from the target permitted 90° stereo photography of the tracks of incident pions and the charged decay products in addition to photographs of the spectrometer. The entire spark-chamber array was triggered by a counter arrangement similar to that first used by Cronin and Overseth¹⁰ which selected those events in which a pion enters the target, no charged secondaries emerge from the target, and charged decay particles are produced further downstream.

During the experiment 6.2×10^5 photographs were taken. Data taken at the three central momentum settings of 0.910, 0.926, and 1.040 GeV/c were subdivided into 1-MeV/c momentum intervals according to the momentum determination obtained with the spectrometer, whereas the remaining momentum settings were treated as single data points. In order to compute cross sections, beam-momentum profiles were determined at the 0.910-, 0.926-, and 1.040-GeV/c settings by also measuring momenta for events in which the beam particle did not interact in the hydrogen target, but did interact in the range chamber. These beam-track events represented "leakage" through the anticoincidence counter following the hydrogen target and were uniformly distributed throughout the same film in which the ΛK events were located. This procedure permitted study of the entire region from threshold to 1.135 GeV/c with enhanced precision in momentum near threshold and in the region of the ΣK thresholds.

All film was scanned twice with overall scanning efficiency of 99% and measured on a preci-